



## International Journal of Current Research and Academic Review

ISSN: 2347-3215 Volume 4 Number 8 (August-2016) pp. 30-44

Journal home page: <http://www.ijcrar.com>

doi: <http://dx.doi.org/10.20546/ijcrar.2016.408.003>



### Green Synthesis and Characterization of Iron Oxide Nanoparticles using *Wrightia tinctoria* Leaf Extract and their Antibacterial Studies

M. Sravanthi<sup>1</sup>, D. Muni Kumar<sup>1</sup>, M.Ravichandra<sup>2</sup>, G.Vasu<sup>1</sup> and K.P.J. Hemalatha<sup>1,2\*</sup>

<sup>1</sup>Department of Biochemistry, Andhra University, Visakhapatnam– 530 003, India

<sup>2</sup>Advanced Analytical Laboratory, DST-PURSE, Andhra University, Visakhapatnam–530 003, India

\*Corresponding author

#### KEYWORDS

Green synthesis, Iron oxide nanoparticles, *Wrightia tinctoria*, characterization, X-ray diffraction, Fourier transform infrared spectroscopy (FT-IR), antibacterial activity.

#### A B S T R A C T

The synthesis of nanoparticles has become a matter of great interest in recent times due to their various advantageous properties and applications in a variety of fields. Recently, the exploitation of different plant materials for the biosynthesis of nanoparticles is considered a green technology because it does not involve any harmful chemicals. Among them, Iron nanoparticles (Fe NPs) are gaining importance for their use in environmental remediation technologies. In the present study, iron oxide nanoparticles (Fe<sub>3</sub>O<sub>4</sub>-NPs) were synthesized using a rapid, single step and completely green biosynthetic method by reduction of ferric chloride solution with *Wrightia tinctoria* leaf extract which acts as reducing agent and efficient stabilizer at room temperature. Synthesized nanoparticles were characterized using UV-visible spectrophotometer FT-IR, X-ray diffraction and SEM methods. The morphology of the nanoparticles mostly appeared to be porous and spongy, nanoclusters with panoramic view and range from 105-145 nm in size. X-ray diffraction showed that the nanoparticles are crystalline in nature, with a cubic shape and rhombohedral geometry. The synthesized Iron oxide nanoparticles exhibited potent antibacterial activity against gram positive and moderate activity against gram negative bacterial strains tested. Novelty of this present study is that the plant extract is very cost effective and eco friendly and thus can be economic and effective alternative for the large scale synthesis of iron oxide nanoparticles.

#### Introduction

Nanotechnology can be defined as the manipulation of matter through certain chemical and/or physical processes to create materials with specific properties, which can

be used in particular applications. A nanoparticle can be defined as a microscopic particle that has at least one dimension less than 100 nanometers in size (Thakkar *et al.*,

2010). Unlike bulk materials, they have unique optical, thermal, electrical, chemical and physical properties (Panigrahi *et al.*, 2004) and hence, they find a variety of applications in the areas of medicine, chemistry, environment, energy, agriculture, information, and communication, heavy industry, and consumer goods. Nanoparticles, because of their small size, have distinct properties compared to the bulk form of the same material, thus offering many new developments in the fields of biosensors, biomedicine and bionanotechnology.

Nanotechnology is also being utilized in medicine for diagnosis, therapeutic drug delivery and for the development of treatment for many diseases and disorders specifically in the areas of drug delivery, as medical diagnostic tools, as cancer treatment agents (Gold, Cu, Fe nanoparticles) etc. During the last two decades, the biosynthesis of metal nanoparticles (silver, copper, iron, gold, platinum and palladium) has received considerable attention due to the growing need to develop environmentally sociable technologies in material synthesis.

The biological synthesis of nanoparticle is a challenging concept which is very well known as green synthesis. Biosynthesis of nanoparticles could be an alternative to traditional chemical methods for the production of metallic nanomaterials in a clean, nontoxic and ecologically sound manner. Green synthesis of nanoparticle is cost effective, easily available, eco friendly, non-toxic, large scale production can be done easily and act as reducing and capping agent when compared to the chemical method which is a very costly as well as emits hazardous by-products which can have some deleterious effects on the environment. Synthesis of nanoparticles using plants provides more biocompatible nanoparticles

than chemical synthesis, whereas chemical synthesis may lead to the presence of some toxic chemical species on the surface of nanoparticles that may have undesirable effects in biomedical applications (Ahmad *et al.*, 2011).

Plant-mediated biological synthesis of nanoparticles has gained importance only in the recent years (Gardia *et al.*, 2002). Plant extracts reduce the metal ions in a shorter time as compared to microbes. Depending upon plant type and concentration of phytochemicals, nanoparticles are synthesized within a few minutes or hours (Rai *et al.*, 2008).

Iron oxide nanoparticles have attracted intensive research interest because of their important applications in cancer therapy, drug delivery, magnetic resonance imaging (MRI) and wastewater treatment (Vicky *et al.*, 2010). Iron-based nanoparticles are of great interest because of low cost, availability and properties possessed are similar to that of other metallic nanoparticles and find applications in heat transfer systems as super strong materials, sensors, antimicrobial, bactericidal agents used to coat hospital equipment and also as catalysts. The biosynthesis of iron oxide nanoparticles of different sizes and shapes has been reported using bacteria (Yeary *et al.*, 2005), fungi (Roh *et al.*, 2006) and plant extract (Senthil *et al.*, 2012).

*Wrightia tinctoria* (Roxb.), Pala indigo plant or dyers' oleander, is a flowering plant species in the genus *Wrightia* found in India belonging to family Apocynaceae distributed in tropical Africa and Asia. The juice of the tender leaves is used efficaciously in jaundice and is reported to possess aphrodisiac, antihelmintic, anti-inflammatory, astringent and antimicrobial properties. Hence, in the present study, iron oxide nanoparticles ( $\text{Fe}_3\text{O}_4$ -NPs) were

synthesized using leaf extract (aqueous) of *Wrightia tinctoria* by reduction of ferric chloride solution which is cost effective and is eco-friendly approach and their antimicrobial potential against selected pathogenic bacterial strains were studied.

## **Materials and Methods**

### **Plant material**

Fresh leaves of *Wrightia tinctoria* were collected from Andhra University campus, Visakhapatnam. The collected leaf material was tightly packed with polyethene bag and then transferred to the laboratory. Then the leaves were washed with distilled water twice and kept under room temperature.

### **Test organisms for Antibacterial studies**

*Bacillus subtilis* (MTCC 121), *Bacillus licheniformis* (MTCC 429), *Staphylococcus aureus* (MTCC 96), *Streptococcus pneumoniae* (MTCC 2672), *Escherichia coli* (MTCC 118), *Klebsiella pneumoniae* (MTCC 2405), *Pseudomonas aeruginosa* (MTCC 424), *Sphingomonas sanguinis* (MTCC 5495) were collected from Microbial Type Culture Collection (MTCC), Institute of Microbial Technology, Chandigarh.

### **Preparation of plant leaf extract**

Twenty five grams of *Wrightia tinctoria* leaves were accurately weighed, thoroughly washed under running tap water followed by washing it with double deionised water to remove surface impurities. They were crushed using a mortar and pestle and finely macerated. After homogenization, 100ml of double deionised water was added and heated over a water bath maintained at 80°C for 15 min. The extract obtained was filtered through Whatmann No1 Filter paper (pore

size 25µm) and stored in refrigerator for further experiments.

### **Phytochemical tests**

The plant extract so obtained was subjected to preliminary phytochemical screening as follows.

**Tannins:** To 2 ml of extract, 2 ml of 5% FeCl<sub>3</sub> was added and observed for the formation of yellow brown precipitate.

**Alkaloids:** To a few ml of extract, a drop or two of Mayer's reagent were added by the side of the test tube. A white or creamy precipitate indicates the test as positive.

**Saponins:** A few ml of extract was shaken vigorously and observed for a stable persistent froth. The frothing was mixed with few drops of olive oil and shaken vigorously after which it was observed for the formation of an emulsion.

**Terpenoids:** To 2 ml of extract, 5 ml CHCl<sub>3</sub>, 2 ml acetic anhydride, and concentrated H<sub>2</sub>SO<sub>4</sub> were added carefully to form layer. Reddish brown coloration of interface was observed to detect the presence of terpenoids.

**Flavonoids:** To 2 ml extract, few drops of concentrated HCl followed by 0.5 g of zinc or magnesium turnings were added. The solution was observed for the appearance of magenta red or pink colour after 3 min.

**Phenolics:** To 2 ml of extract, 1 ml of 1% ferric chloride solution was added. Blue or green colour indicates phenols.

**Test for Anthraquinones:** To 1ml of plant extract, few drops of 10% ammonia solution were added; appearance pink colour

precipitate indicates the presence of anthraquinones.

**Detection of Phytosterols:** To few ml of filtrate, 2 ml acetic anhydride, to this, one or two drops of concentrated sulphuric acid were added slowly along the sides of the test tube. An array of colour changes shows the presence of phytosterols.

**Test for coumarins:** To 1 ml of extract, 1ml of 10% NaOH was added. Formation of yellow colour indicates the presence of coumarins.

**Test for anthocyanins:** To 2ml of extract, 2ml of 2N HCl was added followed by the addition of NH<sub>3</sub>. Pinkish red to bluish violet coloration indicates the presence of anthocyanins.

#### **Synthesis of Iron oxide Nanoparticles using *Wrightia tinctoria* leaf extracts**

1 ml of leaf extract was added to 100 ml of 1mM aqueous FeCl<sub>3</sub>.2H<sub>2</sub>O solution in a 250 ml Erlenmeyer flask (Pattanayak and Nayak, 2013). The flask was then kept stirring for 1hour at room temperature. A change in colour from faint yellow to brownish yellow and finally dark after certain time period indicates the formation of Iron oxide nanoparticles. The Iron oxide nanoparticles solution thus obtained was purified by repeated centrifugation at 12,000 rpm for 15 min followed by re-dispersion of the pellet in deionized water. Then the Iron oxide nanoparticles were dried in oven at 80°C and stored in air tight container for further analysis.

#### **Characterization of Iron oxide Nanoparticles**

##### **UV-spectrophotometer analysis**

The synthesized iron nanoparticles were characterized through Shimadzu UV-1800.

The reduction of iron nanoparticles was monitored by UV-spectrophotometer range of absorbance from 390-600nm in cells with an optical path of 1 cm. The spectra of the intact plant extract were used as a baseline and subtracted from the spectra of a mixture of extracts and synthesized nanoparticles.

##### **FT-IR analysis**

The prepared Iron oxide nanoparticles were then subjected to FT-IR spectroscopy measurements. It was used to identify the possible functional groups of biomolecules responsible for the reduction and capping of the nanoparticles, which are present in the leaf extract. FTIR analysis was carried out for the reduction of Fe ions with the spectral range of 400-4000 cm<sup>-1</sup> using FT-IR Spectrophotometer, Shimadzu, Japan.

##### **Scanning Electron Microscope (SEM-EDX)**

Morphology and mean particle size of the Iron nanoparticles were determined by SEM analysis. The SEM analysis was established by using Scanning Electron Microscope (SEM) Jeol Asia PTE Ltd, Japan with 1nm resolution at 20 kV with 20 mm Oxford, UK, EDS detector. The elemental composition in the reaction mixture was determined by EDX analysis.

##### **X-Ray Diffraction**

The crystalline structure of the Iron nanoparticles was determined by X-Ray diffraction analysis using X-Ray Diffraction Unit (XRD) Pan Alytical, X-Pert pro, Netherlands operating at 40 kV with 2sec time interval at room temperature.

##### **Antimicrobial activity**

##### **Determination of antimicrobial activity**

Active cultures were generated by inoculating a loopful of culture in 100 ml

nutrient broth and incubating on a shaker at 37°C overnight. The cells were harvested by centrifuging at 4000 rpm for 5 min, washed with normal saline, spun at 4000 rpm for 5 min again and diluted in normal saline to obtain  $5 \times 10^5$  CFU/ml.

### **Antibacterial activity**

Antibacterial activity was screened against eight bacterial strains by Agar well diffusion method of Murray *et al.*, (1995) modified by Olurinola (1996).

Nutrient Agar plates were prepared and swabbed using sterile L-shaped glass rod with 100 µl of 24 h mature broth culture of individual bacterial strains. The wells were made by using sterile cork borer (6 mm) wells created into the each Petri-plate. Varied concentrations of Iron oxide nanoparticles (25 and 50 µg/well) were used to assess the activity of the nanoparticles. The nanoparticles were dispersed in sterile water and the standard antibiotic, Ampicillin (20 µg/50 µl) (Hi Media, Mumbai, India) as positive control was tested against the bacterial pathogens. Then the plates were incubated at 37°C for 24 h, the zone of inhibition was measured in millimeter (mm) of the every well and also the values were noted.

### **Minimum inhibitory concentration (MIC) assays**

Minimum Inhibitory Concentration (MIC) of Iron oxide nanoparticles was determined according to the method of Elizabeth (2001).

A series of two fold dilution of Iron oxide nanoparticles, ranging from 100-2000 µg/ml, were prepared. After sterilization, the medium was inoculated with the aliquots of culture containing approximately  $5 \times 10^5$  CFU/ml of each organism of 24 h slant

culture in aseptic condition and transferred into sterile 6 inch diameter petri dishes and allowed to set at room temperature for about 10 min and then kept in a refrigerator for 30 min. After the media was solidified, wells were made and different concentrations of Fe nanoparticles ranging from 100-2000µg/ml were added to the wells of each petri dish. The blank plates were without nanoparticles. Inhibition of the growth of the organism in the plates containing inhibitor was judged by comparison with the growth in the control plates. The MIC was determined as the lowest concentration of the nanoparticle inhibiting visible growth of each organism on the agar plate.

### **Results and Discussion**

Preliminary phytochemical analysis for *Wrightia tinctoria* leaf extract was done using standard test procedures to confirm the availability of active phytochemicals in the aqueous leaf extract. Phytochemical analysis showed the presence of tannins, alkaloids, flavonoids, terpenoids and phenols (Table-1).

### **Synthesis of Iron oxide-Nanoparticles (Visual Inspection)**

In the typical synthesis of iron oxide nanoparticles, *Wrightia tinctoria* leaf extract was added slowly into FeCl<sub>3</sub> solution at room temperature. After adding the leaf extract into FeCl<sub>3</sub> solution, within 3 min, a visible color change was observed, the yellow color aqueous solution of FeCl<sub>3</sub> turned to greenish black indicating the synthesis of Iron oxide nanoparticles (Figure-1).

Generally, the iron oxide nanoparticles have been prepared by strong hydrolysis of iron salts at elevated temperature (Ocana *et al.*, 1999). The plant mediated iron oxide

nanoparticles were prepared at room temperature. Hence the mechanism of study of iron oxide nanoparticles formation is a little difficult. However, the organic compound, which is present in the plant extract acts as a reducing as well as capping or binding agent to form iron oxide nanoparticles. The colour change arise from the excitation of the surface plasman resonance (SPR) phenomenon is typically of iron oxide nanoparticles (Shankar *et al.*, 2004).

### **Characterization of Iron oxide Nanoparticles**

#### **UV-Vis Spectra Analysis**

The optical property of synthesized iron oxide nanoparticles is one of the important characteristics for evaluation of its optical and photo catalytic activity. UV-Visible absorption spectrum is the preliminary characterization to know the optical property. The result obtained from UV-Visible spectroscopy analysis of the sample is presented in Figure-2.

Addition of *Wrightia tinctoria* extract to 0.001 M ferric (III) chloride produced an instantaneous color change in the solution from yellow to intense brown, indicating the formation of iron-containing nanoparticles (Kharissova *et al.*, 2013). This phenotypic change correlated well with the absorption spectra data, such that the absorption peak at 360 nm of the ferric (III) chloride was shifted to 405 nm after the addition of the plant extract, with the 405 nm peak being indicative of iron nanoparticle formation.

In the present study, the absorption maxima of synthesized Iron oxide nanoparticles are similar to those observed in other studies which used tea and sorghum extracts to produce iron nanoparticles (Njagi *et al.*,

2011; Kharissova *et al.*, 2013; Hoag *et al.*, 2009). An absorption maxima of iron nanoparticles with a peak of 415 nm has been reported by Pande *et al.*, (2015), Mazur *et al.*, (2013) and Madhavi *et al.*, (2013).

#### **FTIR analysis**

FTIR spectra of biosynthesized Iron oxide nanoparticles were recorded to identify the capping and efficient stabilization of metal nanoparticles by functional groups of biomolecules present in *Wrightia tinctoria* leaf extract. Figure-3 shows the FT-IR spectrum of prepared iron oxide nanoparticles. It displays three strong bands around  $3468\text{ cm}^{-1}$  (br),  $1626\text{ cm}^{-1}$  and  $548\text{ cm}^{-1}$ . The observed bands are nearer to those reported for Iron nanoparticles (Kumar and Singhal, 2007). The vibration bands are  $548\text{ cm}^{-1}$  (Fe–O stretching),  $1626\text{ cm}^{-1}$  ( $\text{H}_2\text{O}$  bending vibration) and a broad peak at  $3468\text{ cm}^{-1}$  ( $\text{H}_2\text{O}$  stretching) indicating phenolic compounds. Presence of organic molecule on the surface of iron oxide nanoparticles has the influence on the FT-IR peaks (Lee *et al.*, 1996).

The broad peak observed around  $548\text{ cm}^{-1}$  (Fe–O stretching) instead of two sharp peaks, may be due to the organic molecule which was from the leaf extract on the surface of iron oxide nanoparticles. The weak band at  $2074\text{ cm}^{-1}$  may be due to the unsaturated Nitrogen ( $\text{C}\equiv\text{N}$ ) compounds, tannins and alkaloids from the leaf extract. Based on these results, the presence of phenolic compounds, tannins and alkaloids were believed to be responsible for the formation and stabilization of synthesized iron oxide nanoparticles.

In plants, the secondary metabolism products, such as flavonoids, flavones, isoflavones, isothiocyanates, carotenoids, polyphenols that have potent biological

activities are known as an important natural resource for the synthesis of metallic nanoparticles (Park *et al.*, 2011). Flavonoids in *Dodonaea viscosa* leaf extract were identified to be responsible for the reduction of metal salt to synthesize iron oxide nanoparticles along with polyhydroxy groups in santin, tannins and saponins which were considered to be acting as capping agents based on FTIR analysis (Kiruba Daniel *et al.*, 2013). Similarly, the presence of phenols, flavonoids, alkaloids, saponins, cardiac glycosides, steroids, carbohydrate and proteins in *Tinospora cordifolia* were reported to be responsible for the reduction of Ferric ions into nano forms (Pradhan *et al.*, 2013).

Senthil and Ramesh (2012) reported that carbohydrates present in the *Tridax procumbens* plant extract were responsible for Fe<sub>3</sub>O<sub>4</sub> nanoparticle synthesis at room temperature. The phytochemical screening of *Tridax procumbens* revealed the presence of alkaloids, carotenoids, flavonoids, saponins and tannins (Ikewuchi *et al.*, 2009) and reported to be responsible for the Fe<sub>3</sub>O<sub>4</sub> nanoparticle synthesis.

### Scanning Electron Microscope analysis

SEM images revealed that the synthesized iron oxide nanoparticles were aggregated as irregular rhombic shapes with panoramic view and range from 105-145 nm in size (Figure-4).

To find out the purity of the metal particles synthesized, EDX spectrum was obtained. Dispersive X-ray Spectroscopy (EDX) analysis showed the presence of elemental iron oxide signal in the sample (Figure-5). The appearance of chloride and carbon in the EDX spectrum is because of the FeCl<sub>3</sub> precursors used in the synthesis protocol and attributed mainly to organic molecules in the leaf extract.

Iron oxide nanoparticles synthesized by using the leaf extract of *Carica papaya* showed that the synthesized nanoparticles were plate like structures with coarsened grains, uniformly distributed small spherical shaped particles and at higher magnification, large number of homogeneous nanocapsule like morphology of iron oxide nanoparticles were observed (Latha and Gowri, 2014). Pande *et al.*, (2015) reported that the typical SEM image revealed that the iron nanoparticles were clearly distinguishable at different enlargements were found to be polydispersed and measured in size from 24 to 34 nm.

An eco-friendly green synthesis of iron oxide nanoparticles using leaf extract of *Ocimum sanctum* revealed that the particles were aggregated with rough surfaces. Transmission electron microscope image of iron oxide nanoparticles showed that the nanoparticles size was below 20 nm Balamurugan *et al.*, (2014).

### XRD analysis

The phase identification and crystalline structure of the nanoparticles were characterized by X-ray diffraction. The X-ray diffraction patterns obtained for the Fe<sub>3</sub>O<sub>4</sub>-NPs synthesized using *Wrightia tinctoria* extract is shown in Figure 6. The synthesized particles when subjected to XRD analysis, gave a clear picture on the presence of major characteristic peaks for prepared crystalline metallic nanoparticles at  $2\theta$  values of 24.2, 33.1, 35.7, 40.9, 49.4, 54.1, 57.6, 62.6, and 64.0 degrees corresponding to (14), (102), (112), (115), (21), (113), (012), (218), and (298) respectively. In addition, the peak observed at  $2\theta$  values of 45.5 is corresponding to (335). It might be due to the presence of trace amount of hollow  $\gamma$ -Fe<sub>3</sub>O<sub>4</sub> nanoparticles. It indicates that the prepared

iron oxide nanoparticles are well crystalline. Above all, it is encouraging to note that the 2 $\theta$  values of the synthesized iron oxide nanoparticles are also matched with Joint Committee for Powder Diffraction Standard (JCPDS) which are in rhombohedral geometry.

The XRD spectrum obtained with the Iron oxide nanoparticles synthesized using *Ocimum sanctum* leaf extract showed three different diffraction peaks corresponding to the crystal planes of crystalline Fe<sub>2</sub>O<sub>3</sub>. The sharp peaks indicated the crystallinity and purity of iron oxide nanoparticles (Balamurugan *et al.*, 2014). The crystalline structure of iron oxide nanoparticles has also been reported by Pravallika *et al.*, (2015), where they synthesized iron oxide nanoparticles by using *Centella asiatica* extracts.

Phumying *et al.*, (2013) reported the synthesis Fe<sub>3</sub>O<sub>4</sub> nanoparticles using Aloe vera plant extract and high purity of synthesized nanoparticles was confirmed with XRD. The average particle size calculated from XRD increased with an increase in temperature and time. Based on the cocercivity, it was concluded that the nanoparticles were superparamagnetic in nature.

### **Antibacterial activity of Iron oxide nanoparticles**

The antibacterial properties of the Iron oxide Nanoparticles were evaluated against four Gram positive and four Gram negative bacterial strains using agar well diffusion method (Figure-7). Table -2 shows the effect of Iron oxide nanoparticles on the growth of both Gram positive and Gram negative bacteria. Iron oxide nanoparticles exhibited significant antibacterial activity against Gram positive bacteria than Gram negative pathogenic bacterial strains tested.

Of the bacterial stains tested, Iron oxide nanoparticles strongly inhibited the growth of Gram positive bacteria - *Bacillus subtilis* (25 mm), *Bacillus licheniformis* (21 mm), *Streptococcus pneumoniae* (24 mm) and *Staphylococcus aureus* (25mm) at a concentration of 50  $\mu$ g. On the other hand, Iron oxide nanoparticles moderately inhibited the growth of Gram negative bacteria- *Escherichia coli* (19 mm) and *Klebsiella pneumoniae* (22 mm) at a concentration of 50  $\mu$ g. These nanoparticles showed a low inhibitory effect on the growth of *Pseudomonas aeruginosa* (12mm) and *Sphingomonas sanguinis* (11 mm). Hence, the nanoparticles are less susceptible to *Pseudomonas aeruginosa* and *Sphingomonas sanguinis*.

Minimum inhibitory concentration of Iron oxide Nanoparticles for the antibacterial activities was presented in Table- 3.

Most of the synthetic antibiotics now available in the market have major setback due to the multiple resistance developed by pathogenic microorganisms against their drugs (Akinpelu *et al.*, 2008). The emergence of nanoscience and nanotechnology in the last decade presents opportunities for exploring the bactericidal effect of metal nanoparticles. The bactericidal effect of metal nanoparticles has been attributed to their small size and high surface to volume ratio, which allows them to interact closely with microbial membranes and is not merely due to the release of metal ions in solution (Mohanty *et al.*, 2011).

Kiruba Daniel *et al.*, (2013) used leaf extract of the evergreen shrub *Dodonaea viscosa* to synthesize iron nanoparticles and the antimicrobial activity of synthesized nanoparticles was evaluated against human pathogens, namely, *E. coli*, *K. pneumoniae*, *P. fluorescens*, *S. aureus*, and *B. subtilis*. A

very low concentration of as-synthesized nanoparticles was sufficient to display

effective antimicrobial activity as compared to earlier reports.

**Table.1** Preliminary Phytochemical screening tests of *Wrightia tinctoria* leaf extract

Plant Metabolite	<i>Wrightia tinctoria</i> aqueous extract
Tannins	+
Alkaloids	+
Saponins	-
Terpenoids	+
Flavonoids	+
Phenolics	+
Anthraquinones	-
Phytosterols	-
Coumarins	-
Anthocyanins	-

+ Presence - Absence

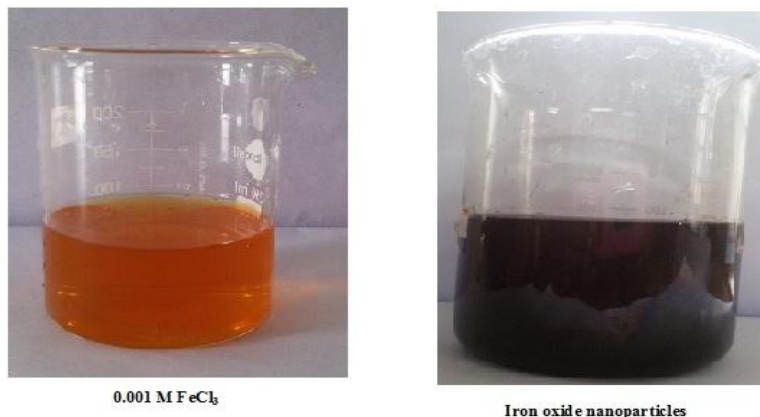
**Table.2** Effect of Iron oxide nanoparticles on the growth of bacteria

Name of the Bacterial strain	Zone of Inhibition (Diameter in mm)		
	Iron oxide Nanoparticles		Ampicillin (20 µg)
	25 µg	50 µg	
<b>Gram positive bacteria</b>			
<i>Bacillus subtilis</i>	15	25	28
<i>Bacillus licheniformis</i>	11	21	27
<i>Streptococcus pneumoniae</i>	11	24	28
<i>Staphylococcus aureus</i>	12	25	28
<b>Gram negative bacteria</b>			
<i>Escherichia coli</i>	10	19	28
<i>Klebsiella pneumoniae</i>	14	22	27
<i>Pseudomonas aeruginosa</i>	8	12	28
<i>Sphingomonas sanguinis</i>	7	11	26

**Table.3** Minimum Inhibitory concentration (MIC) of Iron oxide nanoparticles on bacterial growth

Name of the bacterial strain	Minimum Inhibitory Concentration (MIC) of Iron oxide nanoparticles (µg/ml)
<i>Bacillus subtilis</i>	200
<i>Bacillus licheniformis</i>	250
<i>Streptococcus pneumoniae</i>	200
<i>Staphylococcus aureus</i>	200
<i>Escherichia coli</i>	250
<i>Klebsiella pneumoniae</i>	350
<i>Pseudomonas aeruginosa</i>	400
<i>Sphingomonas sanguinis</i>	500

**Fig.1** Digital photograph of visible color changes, after adding the *Wrightia tinctoria* leaf extract into an aqueous 0.001M Ferric chloride



The yellow color aqueous solution of FeCl<sub>3</sub> turned to greenish black indicating the synthesis of Iron oxide nanoparticles

**Fig.2** Absorption spectra of iron oxide nanoparticles (red line) and 0.001 M aqueous solution of FeCl<sub>3</sub> (blue line)

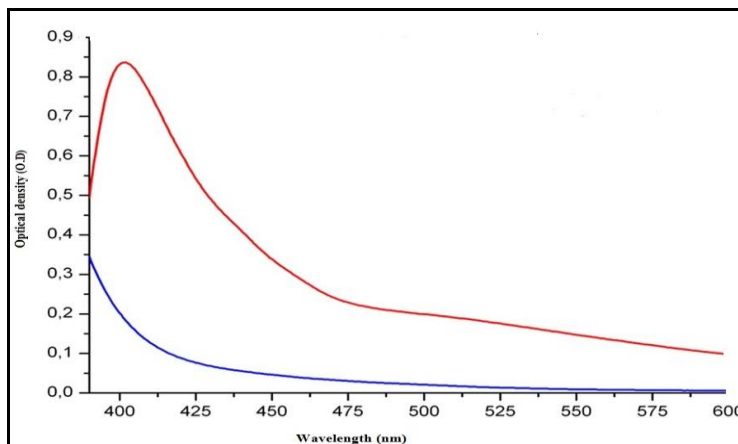
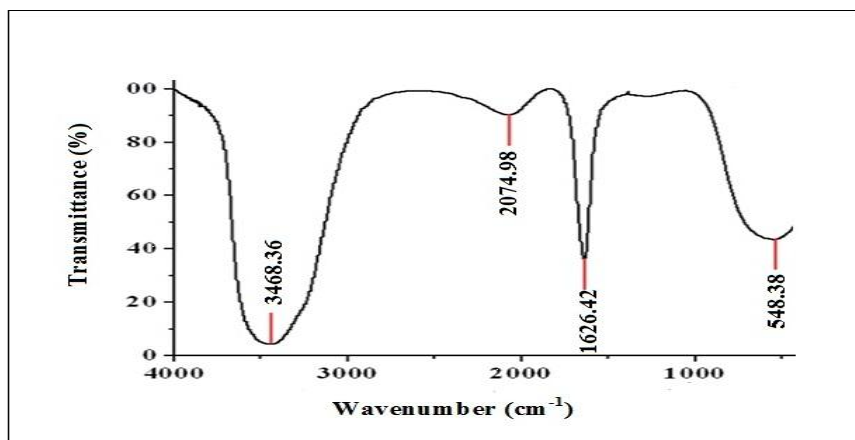


Fig.3 Fourier Transform Infra Red spectroscopy of iron oxide Nanoparticles



FT-IR spectrum of synthesized iron oxide nanoparticles

Fig.4 SEM images of synthesized Iron oxide nanoparticles at different resolutions

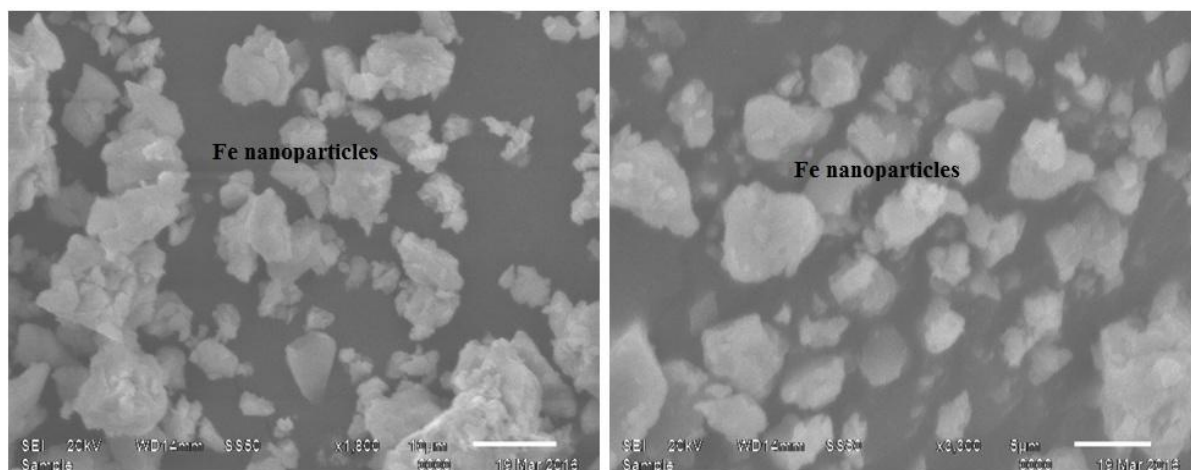


Fig.5 EDX analysis showing synthesized Iron nanoparticles

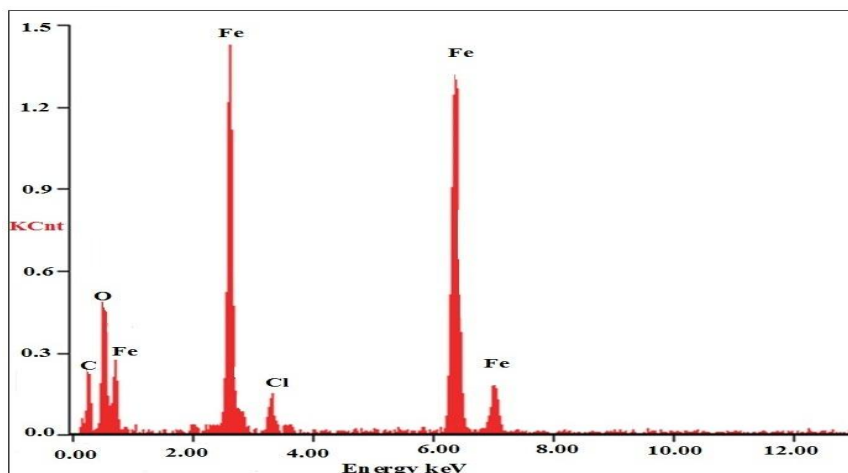


Fig.6 XRD spectrum of synthesized iron oxide nanoparticles

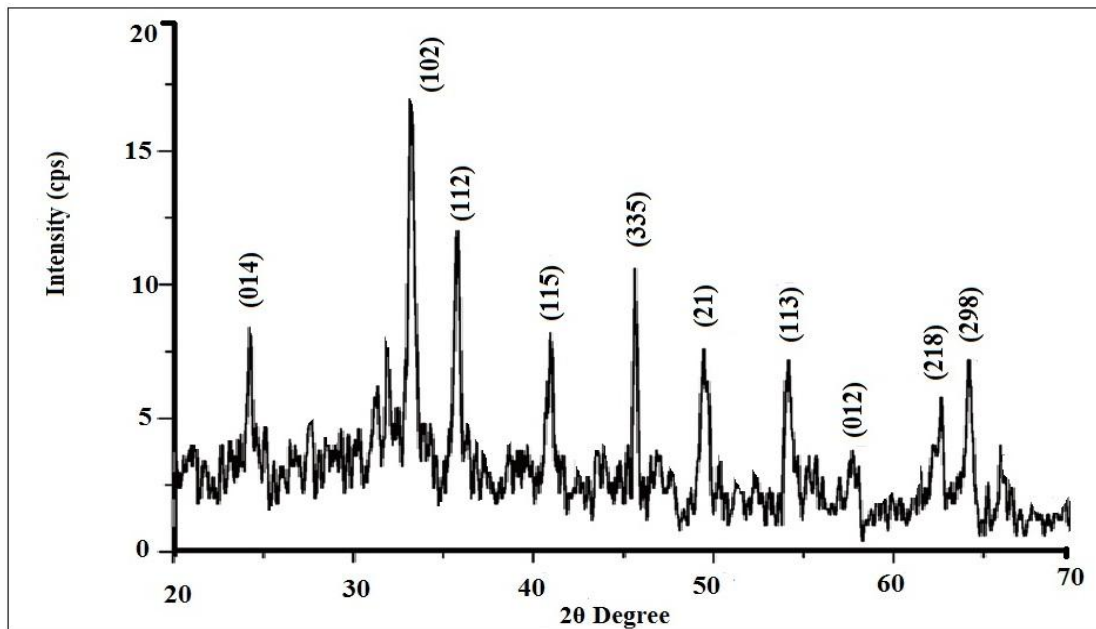
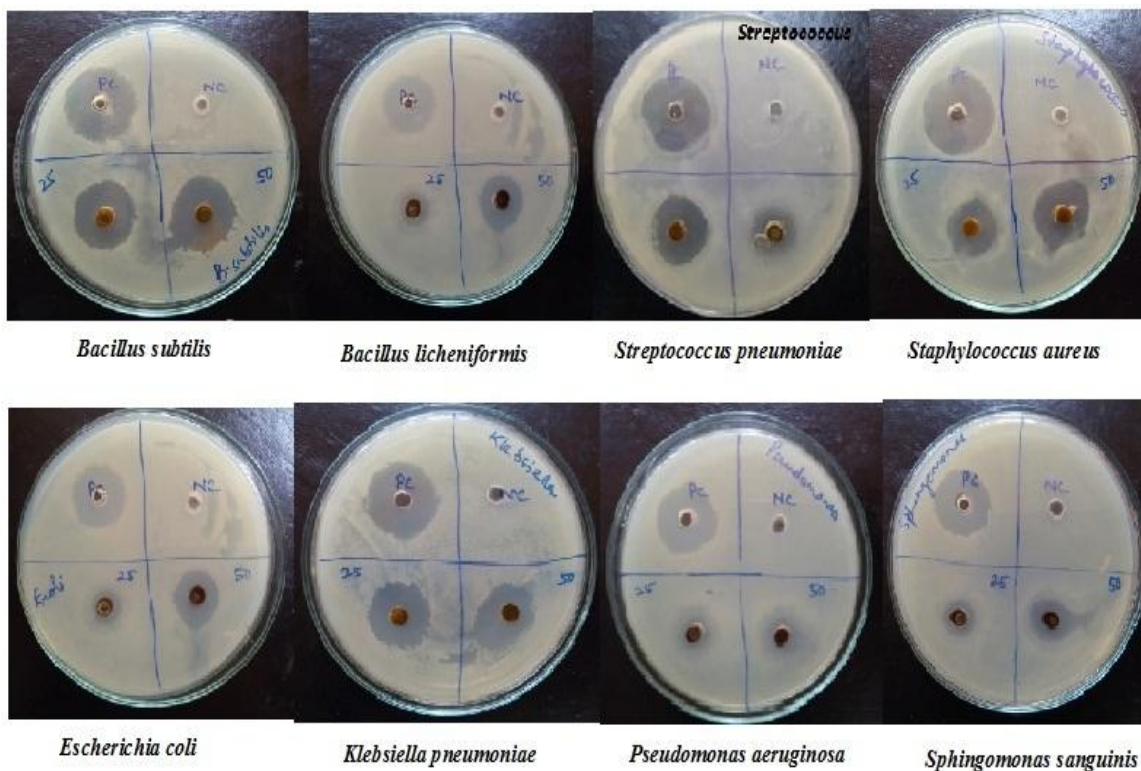


Fig.7 Effect of Iron oxide nanoparticles on the growth of bacteria



Senthil and Ramesh (2012) reported the green synthesis of  $Fe_3O_4$  nanoparticles at room temperature using leaf extract of

*Tridax procumbens* and the synthesized nanoparticles were effective against *Pseudomonas aeruginosa*. The zone of

inhibition increased from 1mm to 2mm when the concentration of nanoparticles increased four fold.

Nanoparticles prepared by using *Abelmoschus esculentus* as a reducing and capping agent significantly inhibited the growth of *Escherichia coli* and *Staphylococcus aureus* (Pande *et al.*, 2015).

Bacterial strains were spread on agar plates. Different amounts of Fe<sub>3</sub>O<sub>4</sub> nanoparticles (25 µg & 50 µg) were placed in the wells. Controls contained Ampicillin (20µg) in place of Fe<sub>3</sub>O<sub>4</sub> nanoparticles. The incubation period was 24 h at 37°C. Zone of inhibition was measured as described in methods.

Bacterial strains were spread on agar plates. Different concentrations of Iron oxide nanoparticles (0.1-2.0 mg/ml) were placed in the wells. Control contained Ampicillin (20µg) in the place of nanoparticles. The incubation period was 24 h at 37°C. Zone of inhibition was measured and minimum inhibitory concentration of Iron oxide nanoparticles was determined.

### **Conclusion**

In the present study, the biological approach of synthesis of Iron oxide nanoparticles using *Wrightia tinctoria* leaf extract appears to be ecofriendly and cost effective alternative to conventional chemical and physical methods and would be suitable for developing large-scale production. The characteristics of the obtained Fe<sub>3</sub>O<sub>4</sub> nanoparticles were studied using UV-Visible spectrophotometer, FTIR, SEM with EDX and XRD. The synthesized Iron oxide nanoparticles were effectively utilized for the antibacterial activity study. The maximum zone of inhibition was found to be high in Gram positive bacteria when compared to Gram negative bacteria. This

green method of synthesizing Fe<sub>3</sub>O<sub>4</sub> nanoparticles could also be extended to fabricate other industrially important metal oxides. This simple, low cost and greener method for development of nanoparticles may be valuable in environmental, biotechnological and biomedical applications.

### **Acknowledgements**

We gratefully acknowledge Advanced Analytical Laboratory (AAL), DST-PURSE Programme, Andhra University for assisting in getting FTIR, SEM-EDX and XRD analysis for the iron oxide nanoparticles.

### **References**

- Ahmad, N., Sharma, S., Singh, V.N., Shamsi, S.F., Fatma, A., Mehta, B.R. 2011. Biosynthesis of Silver Nanoparticles from *Desmodium triflorum*: a novel approach towards weed utilization.,” *Biotech. Res. Int.* 1-8.
- Akinpelu, D.A., Aiyegoro, O.A., Okoh, A.I. 2008. *In vitro* antimicrobial and phytochemical properties of stem bark of *Azelia africana* (Smith). *Afri. J. Biotech.*, 7(20): 3665 -3670.
- Balamurugan, M.G., Mohanraj, S., Kodhaiyolii, S., Pugalenti, V. 2014. *Ocimum sanctum* leaf extract mediated green synthesis of iron oxide nanoparticles. Spectroscopic and microscopic studies. *J. Chem. Pharm. Sci.*, 4: 201–204.
- Elizabeth, M., Adrien Szekely, Johnson., David Warnock, W. 2001. Comparison of E-Test and broth microdilution methods for antifungal drug susceptibility testing of molds. *J. Clin. Microbiol.*, 37(5): 1480-1483.
- Gardea-Torresdey, J.L., Parsons, J.G., Gomez, E. 2002. Formation and

- growth of Au nanoparticles inside live Alfalfa plants. *Nano Lett.*, 2(4): 397–401.
- Hoag, G., Collins, A., Holcomb, J., Hoag, J., Nadagouda, M., Varma, R. 2009. Degradation of bromothymol blue by ‘greener’ nano-scale zero-valent iron synthesized using tea polyphenols. *J. Mater. Chem.*, 19: 8671–8677.
- Ikewuchi, J.C., Ikewuchi, C.C., Igboh, M.N. 2009. Chemical profile of *Tridax procumbens* Linn. *Pak. J. Nutr.*, 8(5): 548-550.
- Kharissova, O.V., Dias, H.V., Kharisov, B.I., Pérez, B.O., Pérez, V.M. 2013. The greener synthesis of nanoparticles. *Trends Biotechnol.*, 31(4): 240–248.
- Kiruba Daniel, S.C.G., Vinothini, G., Subramanian, N., Nehru, K., Sivakumar, M. 2013. Biosynthesis of Cu, ZVI and Ag nanoparticles using *Dodonaea viscosa* extract for antibacterial activity against human pathogens. *J. Nano Res.*, 15(1):1-10.
- Kumar, A., Singhal, A. 2007. Synthesis of colloidal  $\beta$ -Fe<sub>2</sub>O<sub>3</sub> nanostructures-influence of addition of Co<sup>2+</sup> on their morphology and magnetic behavior. *Nanotechnol.*, 18(47): 1-7.
- Latha, N., Gowri, M. 2014. Biosynthesis and characterization of Fe<sub>3</sub>O<sub>4</sub> nanoparticles using *Carica papaya* leaves extract. *Int. J. Sci. Res.*, 3(11): 1551-1556.
- Lee, Jiwon., Tetsuhiko, Isobe., Mamoru, Senna. 1996. Preparation of ultrafine Fe<sub>3</sub>O<sub>4</sub> particles by precipitation in the presence of PVA at high pH. *J. Coll. Inter Sci.*, 177(2): 490-494.
- Madhavi, V., Prasad, T.N.V.K.V., Reddy, A.V B., Ravindra Reddy, B., Madhavi, G. 2013. Application of phytogenic zerovalent iron nanoparticles in the adsorption of hexavalent chromium. *Spectrochimica Acta A: Mol. Biomol. Spectro.*, 116:17–25.
- Mazur, M., Barras, A., Kuncser, V., Galatanu, A., Zaitzev, V., Turcheniuk, K.V., Woisel, P., Lyskawa, J., Laure, W., Siriwardena, A., Boukherroub, R., Szunerits, S. 2013. Iron oxide magnetic nanoparticles with versatile surface functions based on dopamine anchors. *Nanoscale.*, 5:2692–2702.
- Mohanty, L., Parida, U.K., Ojha, A.K, Nayak, P.L. 2011.Green synthesis of Gold nanoparticle using *Elettaria cardamomum* seed extract. *J. Micro Antimicro.*, 3:105-109.
- Murray, P.R., Baron, E.J., Pfaller, M.A., Tenover, F.C., Tenover, H.R. 1995. Manual of Clinical Microbiology. 6th Edition, ASM Press, Washington DC. 15-18.
- Njagi, E.C., Huang, H., Stafford, L., Genuino, H., Galindo, H.M., Collins, J.B., Hoag, G.E., Suib, S.L. 2011. Biosynthesis of iron and silver nanoparticles at room temperature using aqueous sorghum bran extracts. *Langmuir.*, 27(1): 264-271.
- Ocana, M, Morales, M.P., Serna, C.J. 1999. Homogeneous precipitation of uniform  $\alpha$ -Fe<sub>2</sub>O<sub>3</sub> particles from iron salts solutions in the presence of urea. *J. colloid inter sci.*, 212 (2): 317-323.
- Olurinola, P.F. 1996. A laboratory manual of pharmaceutical microbiology. Idu, Abuja, Nigeria, 69- 105.
- Nishigandh, Pande S., Dipika Kaur, Jaspal., Arti, Malviya., Jayachandran, V.P. 2015. Green route synthesis of iron nanoparticles and antibacterial studies. *Int. J. Adv. Sci. Engg Technol.*, 3(2): 98-102.
- Panigrahi S., Kundu, S., Ghosh, S.K., Nath, S., Pal, T. 2004. General method of synthesis for metal nanoparticles. *J. Nanoparticle Res.*, 6(4): 411–414.
- Park, Y., Hong, Y.N., Weyers, A., Kim, Y.S., Linhardt, R.J. 2011.

- Polysaccharides and phytochemicals: a natural reservoir for the green synthesis of gold and silver nanoparticles. *IET Nanobiotechnol.*, 5: 69-78.
- Pattanayak, M., Nayak, P.L. 2013. Green synthesis and characterization of zero valent Iron nanoparticles from the leaf extract of *Azadirachta indica* (Neem). *World J. Nano Sci. Technol.*, 2(1): 06-09.
- Phumying, S., Labuayai, S., Thomas, C., Amornkitbamrung, V., Swatsitang, E., Maensiri, S. 2013. Aloe vera plant-extracted solution hydrothermal synthesis and magnetic properties of magnetite (Fe<sub>3</sub>O<sub>4</sub>) nanoparticles. *Applied Physics A.*, 111(4):1187–1193.
- Pradhan, D., Ojha, V., Pandey, A.K.2013. Phytochemical analysis of *Tinospora cordifolia* (willd.) miers ex hook. f. & thoms stem of varied thickness. *IJPSR.*, 4(8): 3051-3056.
- Pravallika, Lakshmi P., Krishna Mohan, G., Venkateswara Rao, K. 2015. Green synthesis and characterization of iron oxide magnetic nanoparticles using *Centella asiatica* plant-a theranostic agent. *Int. J. Eng. Res.*, 3: 52-59.
- Rai, M., Yadav, A., Gade, A. 2008. CRC 675—current trends in phytosynthesis of metal nanoparticles. *Critic. Rev. Biotechnol.*, 28(4): 277–284.
- Roh, H., Vali, T., Phelps, J., Moon, J.W. 2006. Extracellular synthesis of magnetite and metal-substituted magnetite nanoparticles, *J. Nanosci Nanotechnol.*, 6:3517-3520.
- Senthil, M., Ramesh, C. 2012. Biogenic synthesis of Fe<sub>3</sub>O<sub>4</sub> nanoparticles using *Tridax procumbens* leaf extract and its antibacterial activity on *Pseudomonas aeruginosa*. *J. Nanomat. Biostruc.*, 7: 1655-1660.
- Shankar, S.S., Rai, A., Ankamwar, B., Singh, A., Ahmad, A., Sastry, M. 2004. Biological synthesis of triangular gold nanoprisms. *Nat. Mater.*, 3(7): 482-488.
- Thakkar, K.N., Mhatre, S.S., Parikh, R.Y. 2010. Biological synthesis of metallic nanoparticles. *Nanomedicine.*, 6(2): 257–262.
- Vicky, M., Rodney, S., Ajay, S., Hardik, M. 2010. Introduction to metallic nanoparticles. *J. Pharm. Bioallied Sci.*, 2(4): 282-289.
- Yeary, L.W., Ji, W.M., Love, L.J., Thompson, J.R., Rawn, C., Phelps, J., Tommy, J. 2005. Magnetic properties of biosynthesized magnetite nanoparticles, *Magnetics, IEEE Transac.*, 41: 4384-4389.

**How to cite this article:**

Sravanthi, M., D. Muni Kumar, M.Ravichandra, G.Vasu and Hemalatha, K.P.J. 2016. Green Synthesis and Characterization of Iron Oxide Nanoparticles using *Wrightia tinctoria* Leaf Extract and their Antibacterial Studies. *Int.J.Curr.Res.Aca.Rev.4(8): 30-44*.  
doi: <http://dx.doi.org/10.20546/ijcrar.2016.408.003>